Annals of Anatomy 249 (2023) 152094

Contents lists available at ScienceDirect

Annals of Anatomy

journal homepage: www.elsevier.com/locate/aanat

Dual effect of RYGB on the entero-insular axis: How GLP-1 is enhanced by surgical duodenal exclusion

Gonzalo-Martín Pérez-Arana [a,c,*], Alfredo Díaz-Gómez [e], Alonso Camacho-Ramírez [b,c], Antonio Ribelles-García [a], David Almorza-Gomar [c,d], Manuel Gracia-Romero [a], Isabel Mateo-Gavira [f], María-Jesús Castro-Santiago [b], Juan Casar-García [a], José-Arturo Prada-Oliveira [a,c,*]

[a] Department of Human Anatomy and Embryology, University of Cadiz, Spain
[b] Surgery Unit, Puerta del Mar Universitary Hospital, University of Cadiz, Spain
[c] Institute for Biomedical Science Research and Innovation (INIBICA) University of Cadiz, Spain
[d] Operative Statistic and Research Department, University of Cádiz, Spain
[e] San Carlos Hospital, Andalusian Health System, Spain
[f] Endocrinology Unit, Puerta del Mar Universitary Hospital, University of Cadiz, Spain

ARTICLE INFO

Article history:
Received 23 September 2022
Received in revised form 14 March 2023
Accepted 16 March 2023
Available online 1 April 2023

Keywords:
Pancreas
Roux-en-Y Gastric Bypass
Type 2 Diabetes mellitus
Bariatric surgeries
GLP-1

ABSTRACT

Background: The role of the ileum and Glucagon Like Peptide-1 (GLP-1) secretion in the pathophysiological processes underlying the effects of Roux-en-Y gastric bypass (RYGB) on type 2 Diabetes mellitus (T2DM) improvement has been previously determined. However, the roles of duodenal exclusion and Glucose Insulinotropic Peptide (GIP) secretion change is not clear. To clarify this aspect, we compared the pathophysiological mechanisms triggered by RYGB, which implies the early arrival of food to the ileum with duodenal exclusion, and through pre-duodenal ileal transposition (PdIT), with early arrival of food to the ileum but without duodenal exclusion, in a nondiabetic rodent model. Methods: We compared plasma and insulin, glucose (OGTT), GIP and GLP-1 plasma levels, ileal and duodenal GIP and GLP-1 tissue expression and beta-cell mass for n = 12 Sham-operated, n = 6 RYGB-operated, and n = 6 PdIT-operated Wistar rats. Results: No surgery induced changes in blood glucose levels after the OGTT. However, RYGB induced a significant and strong insulin response that increased less in PdIT animals. Increased beta-cell mass was found in RYGB and PdIT animals as well as similar GLP-1 secretion and GLP-1 intestinal expression. However, differential GIP secretion and GIP duodenal expression were found between RYGB and PdIT. Conclusion: The RYGB effect on glucose metabolism is mostly due to early ileal stimulation; however, duodenal exclusion potentiates the ileal response within RYGB effects through enhanced GIP secretion.

1. Background

Bariatric/metabolic surgery has become one of the most powerful tools against type 2 Diabetes mellitus (T2DM) (Schauer et al., 2017) and permits high rates of disease remission with high levels of patient safety (Arterburn et al., 2020). Since the first interventions were conducted, many technical variants involving different elements of the digestive system have been developed (Rahman and Azagury, 2017). One of the most performed procedures is Roux-en-Y gastric bypass (RYGB), which affects the ileum (the terminal portion of the small intestine) and shows the highest T2DM resolution rates (Kalinowski et al., 2017). To explain the pathophysiologic mechanism underlying this phenomenon, many theories have been proposed regarding the key role in Glucagon Like Peptide-1 (GLP-1) secretion by ileal L-cells (Liu et al., 2011) derived from the early arrival of nutrients to the ileum and the anatomical rearrangement after the surgical procedure (Camacho-Ramírez et al., 2020). However, these theories become controversial if we attempt to achieve glucose-level restoration in RYGB-operated GLP-1-deficient diabetic mice (Mokadem et al., 2013).

Additionally, duodenal exclusion of the nutrient flow after RYGB appears to increase the circulating levels of Glucose Insulinotropic Peptide (GIP) in diabetic GK rats (Miskelly et al., 2021). This is an interesting point if we consider the GIP synergistic insulinotropic effects established with GLP-1 in cultured diabetic and nondiabetic

* Corresponding authors at: Department of Human Anatomy and Embryology, University of Cadiz, Spain.
E-mail addresses: gonzalo.perez@uca.es (G.-M. Pérez-Arana), arturo.prada@uca.es (J.-A. Prada-Oliveira).

https://doi.org/10.1016/j.aanat.2023.152094

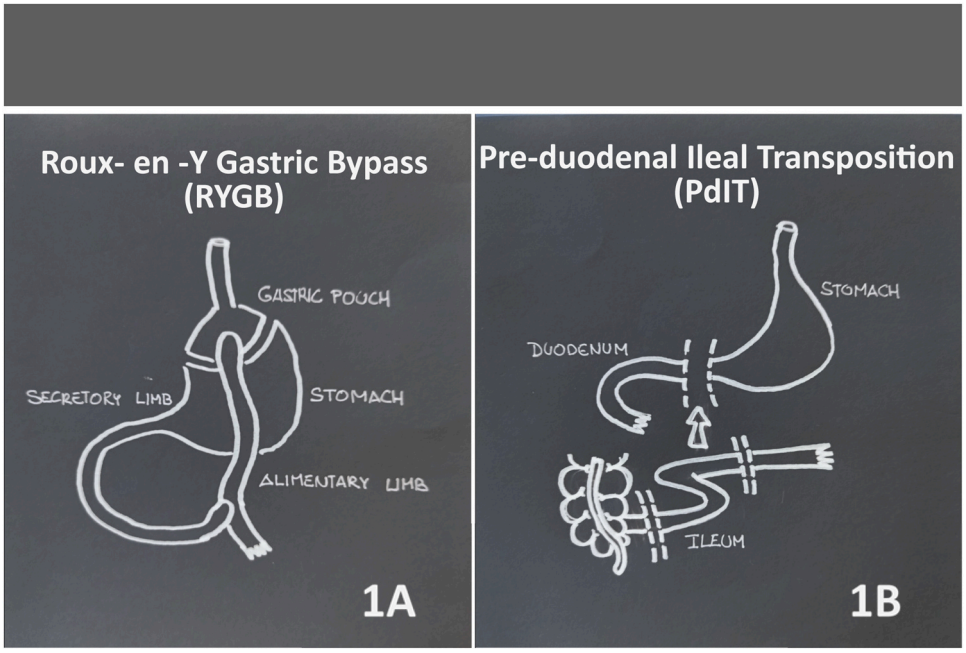

Fig. 1. Schematic drawing of RYGB (Fig. 1A) and PdIT (Fig. 1B) In Fig. 1A we observe the secretory limb formed by the duodenum and the first portion of the jejunum (14 cm from the angle of Treitz) Also the alimentary limb formed by the portion of the jejunum transposed from the junction with the gastric pouch to its junction with the secretory limb. B shows the interposition of the terminal 10 cm of the ileum (1 cm from the ileocecal valve) in the pre-duodenal position.

human islets (Lupi et al., 2010). Moreover, beta-cell GIP resistance due to cell stress has been described in T2DM patients and leads to the consideration of the minor role of the ileum in diabetes resolution after RYGB (Piteau et al., 2007).

Thus, determining which of the two segments of the intestine, the duodenum or ileum, is mainly responsible for the beneficial effects of RYGB is very complex because the absence or early presence of nutrients occurs at the same time in both. To separate these effects, we developed a surgical nondiabetic rat model that permits the early presence of food in the ileum without exclusion of the duodenum from the flux. For this purpose, we performed a preduodenal transposition of the ileum in the animals, called PdIT, by focusing our study on pathophysiological changes in the entero-insular axis derived from the early arrival of nutrients to the ileum with RYGB or without PdIT duodenal exclusion.

2. Research and design methods

2.1. Animal handling and surgical procedures

In this study, all animal procedures were approved by The Committee for Ethical Use and Care of Experimental Animals at Cadiz University. Twenty-four 11-week-old male Wistar rats weighing 210–220 g were provided and kept at the Experimentation and Animal Production Service of the University of Cadiz (SEPA).

2.2. Research protocol

The twenty-four Wistar rats were randomly divided into four groups as follows: n = 6 Sham 1-operated rats (Sham 1), n = 6 Sham 2- operated rats (Sham 2), n = 6 Roux-en-Y gastric bypass-operated rats (RYGB), and n = 6 preduodenal ileal transposition-operated rats (PdIT). All animals were sacrificed twelve weeks after surgery. Each animal in every group finished a 12 h presurgical and 12 h postsurgical fasting period. An intake readaptation period followed surgery to normalize fasting and weight measurement occurred every two days from surgery to the fourth day of survival. Oral Glucose Tolerance Test (OGTT), insulin measurement, and hormonal determinations after meals were also performed over twelve weeks.

2.3. Surgical procedures

The surgical procedures were performed in anaesthetized animals using continuous infusion of isoflurane 2–5 % V/V (Abbott Columbus, OH, USA).

The first sham technique (Sham 1) reproduced a surgical injury over the stomach and gut, but the Sham maintained its integrity. Sham was performed with a laparotomy of 5 cm in the upper third of the abdomen. An incision of approximately 3 cm was made in the middle area of the abdomen and sectioning the gastrosplenic ligament and exposing the stomach occurred. In addition, the jejunum was transected 40 cm distal to the angle of Treitz, and terminus-terminus anastomosis was also performed. Finally, the abdominal muscular and skin layers were closed into one layer using a continuous suturing technique.

The second Sham group (Sham 2) (n = 6) was performed by a laparotomy of 5 cm in the upper third of the abdomen, through sectioning of the gastrosplenic ligament and exposing the stomach too but this time a curved forceps was applied from the angle of Hiss to the end of stomach-corpus. The stomach sectioned resected the most fundus and much of the stomach-corpus at greater curvature. The Sham 2 surgery reduced the initial stomach volume by approximately 30–35 %.

The RYGB group of rats underwent a laparotomy of 3 cm in the midline of the abdomen, and a gastric pouch with a volume of approximately 30 % of the normal gastric volume was completed. The remnant gastric fundus was anastomosed to the jejunum 14 cm distal from the ligament of Treitz. Then, the abdominal layers were closed as above (Fig. 1).

The PdIT group underwent bisubcostal surgery. The stomach was mobilized for better exposure after liberating the lesser omentum. Then, we measured the last 10 cm of the terminal ileum and divided it while preserving the vascular supply and the distal edge 1 cm away from the ileocaecal valve. Then, a transverse postpyloric

division was made to close the duodenal stump with a running suture using PDS 5/0. The distal duodenal stump was anastomosed to the distal edge of the transposed ileum with interrupted stitches of PDS 5/0. The proximal edge of the ileum was anastomosed to the posterior gastric face using continuous suturing with PDS 5/0 after opening the greater omentum. Finally, the last anastomosis was between the jejunum and terminal ileum with interrupted sutures of PDS 5/0 (Fig. 1).

2.4. Weight gaining

Weight gain was measured in all animals every forty-eight hours from the day of the surgical procedure over forty days and expressed in grams.

2.5. Oral glucose tolerance test (OGTT) and insulin measurement

Ten weeks after surgery, oral glucose tolerance tests (OGTTs) were performed in 12-hour-fasting animals. A 20 % w/v D-glucose solution (2 g/kg) was administered through gavage, and glycaemia was measured using a Glucocard G-Metre 1810 glucometer (Menarini Diagnostics, Italy) in blood samples obtained from rat tails at 0, 30, 60, 90 and 120 min after glucose solution administration. The values obtained were expressed as mg/dl of blood glucose. The glucose area under the curve (AUC) was calculated using the trapezoidal rule and expressed as mg/dl min^{-1}.

Insulin measurements were performed ten weeks after surgery in blood samples from rat tails every 15 min for 60 min after the administration of the glucose solution using an ELISA kit (ALPCO Diagnostics, Salem, NH). The values obtained were expressed as μU/ml. Additionally, the insulin area under the curve (AUC) was calculated using the trapezoidal rule and expressed as μU/ml min^{-1}.

2.6. Hormonal determinations

Nine weeks after surgery procedures, a 4 ml/kg 13,9 kJ/ml mixed meal was administered to 12-hour-fasting animals by oral gavage. Blood samples were obtained from Sham 1 and Sham 2, RYGB, and PdIT rat tails every 15 min for 120 min and were added to EDTA tubes containing dipeptidyl peptidase-4 (DPP-4) inhibitor (10 μl/ml) (Millipore, USA) and centrifuged at 4000 x g for 15 min at 4 °C. The plasma fraction was removed and stored at − 80 °C. Plasma concentrations of GIP and GLP-1 were detected using an ELISA kit (ALPCO Diagnostics, Salem, NH) according to the manufacturer's instructions and expressed as pmol/ml.

The GIP and GLP-1 areas under the curve (AUCs) were also determined by the trapezoidal rule and expressed as pmol/ml Min^{-1}.

2.7. Sacrifice and tissue preparation

The animals were sacrificed twelve weeks after surgery using an isoflurane inhalation overdose procedure. Pancreas and gut samples were immediately removed and fixed in Bouin's solution overnight at 4 °C. Later, samples were dehydrated, embedded in paraffin, and cut into 8 μm microtome sections.

2.8. Pancreas immunostaining and beta-cell mass calculation

For rehydrated sections of pancreas, the beta-cell mass was assessment by immunostaining using guinea pig anti-insulin IgG antibody with DAB (Sigma Aldrich, St. Louis MO, USA). We analyzed ten fields at each point of study (10x) in complete sections of pancreas using a microscope with a digital camera and Cell-D image analysis software (Olympus, GmbH. Hamburg, Germany). The beta-cell mass value was obtained by multiplying the total pancreas weight x insulin-positive area/total area ratio and expressed in mg.

For histomorphometric study the islets counted in the pancreas sections described above were measured and classified according to their size in each of the groups under study. The results were expressed as percentage of islets in each size interval.

2.9. GIP and GLP-1 gut expression

For rehydrated sections of the duodenum and ileum, GIP and GLP-1 expression was analysed by immunostaining using rabbit anti-GIP and rabbit anti-GLP-1 primary antibodies (Abcam, Cambridge CB4 OFL, UK). Alexa 488 anti-rabbit was used as the secondary antibody (Molecular Probes Inc. Eugene, OR USA). DAPI was used to counterstain the nuclei. To determine the positive cell fraction, the number of GIP- and GLP-1-positive cells and total intestinal areas were quantified in 10 fields per condition. Results were noted under randomized conditions using a single investigator and expressed as the number of GIP- or GLP-1-positive cells/mm^2 of intestine.

Each parameter was measured and noted by a single investigator using a fluorescence microscope with a digital camera and Cell-D image analysis software (Olympus, GmbH. Hamburg, Germany).

2.10. Statistical analysis

Data are presented as the means ± SEMs in the figures and as means +SEMs/SDs in figure legends. For OGTT, GIP/GLP-1/insulin secretion patterns and weight gain, repeated-measures ANOVA (RM-2 W-ANOVA) was conducted. AUCs and histological data were analyzed using One-way ANOVA followed by Tukey's/Bonferroni's test with the help of SPSS V21.0 software to determine statistical significance ($P < 0.05$ (*, #) or $P < 0.01$ (**, ##).

3. Results

3.1. Functional determinations

Weight gain was measured in Sham 1 and 2, RYGB, and PdIT-operated animals. As shown in Fig. 2A, a significant difference occurred for weight gain between the Sham group and RYGB and PDIT groups (#$P < 0.05$) from the second day to the fortieth day of the study. However, no difference was observed between RYGB and PdIT rats during the study.

The OGTT was performed ten weeks after surgical intervention in each group for Sham1, Sham 2, RYGB, and PdIT. There was no difference among the four groups at any time point (Fig. 2B). Thus, the blood glucose AUC was similar for Shams, RYGB, and PdIT animals as shown in Fig. 2C.

Additionally, the insulin response after the glucose challenge was measured in Sham 1, Sham 2, RYGB, and PdIT rats. As shown in Fig. 2D, an increased insulin secretion pattern was observed in RYGB animals with respect to Sham animals (# $P < 0.05$). However, there was no significant difference between the PdIT and Sham insulin secretion patterns at any time.

However, if we observe the insulin release AUC in Fig. 2E, significant differences occur between Sham 1 and Sham 2 AUC and RYGB or PdIT AUC (*$P < 0.05$), but also between RYGB and PdIT AUC values (*$P < 0.05$).

3.2. Hormonal determinations

GIP and GLP-1 plasma levels were measured following mixed-meal administration in blood samples from the rat's tails of each

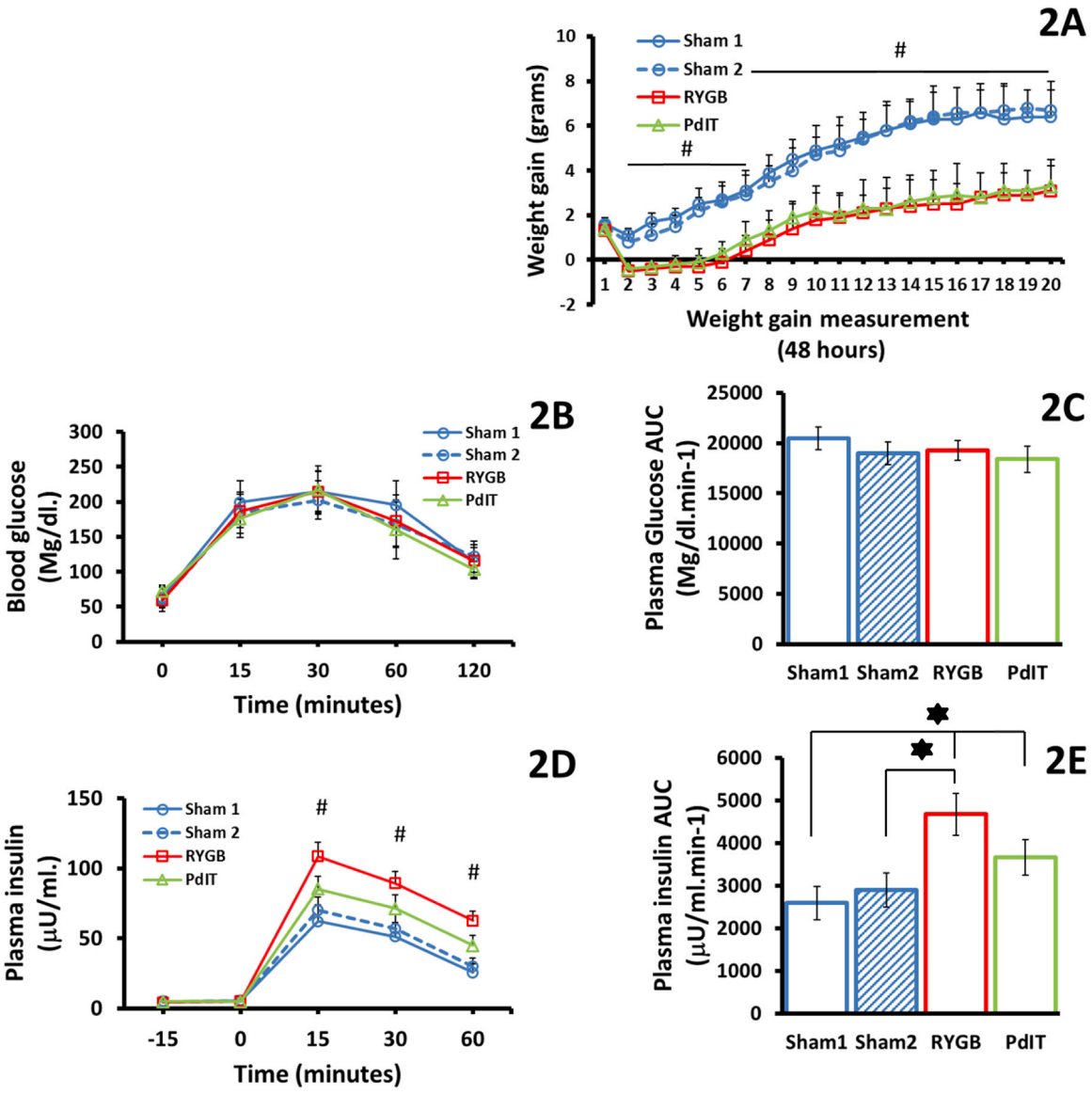

Fig. 2. Functional Study. A, weight gain in n = 6 Sham 1-operated rats; Sham 1(blue line with circles), n = 6 Sham2-operated rats (discontinuous blue line with circles), n = 6 RYGB-operated rats; RYGB (red line with squares) and n = 6 PdIT-operated rats; PdIT (green line with triangles) is presented as grams in the Y axis over forty days following surgery represented in the X axis. Values are expressed as the mean +SEM #P < 0.05. B, Oral glucose tolerance test (OGTT). Glycaemia were represented as mg/dl in the Y axis and time after glucose load in the X axis. Values were expressed as mean +SEM. (#P < 0.05). C, OGTT Area under curve (AUC) values were presented as mg/dl min-1 in the Y axis and expressed as mean +SEM (*P < 0.05) for each group presented in the X axis. Sham 1 (Blue bar), Sham 2 (striped blue bar), RYGB (Red Bar) and PdIT (green bar). Data obtained (mean +SEM/SD): Sham 1: 20,484.52 + 1132.1/2762.32; Sham 2: 18,979.2 + 1124.07/2742.73; RYGB: 19,276.5 + 980.2/2391.68; PdIT: 18,382.04 + 1334.21/3279.87. D, Plasma insulin after glucose challenge. Plasma insulin levels were represented as µU/ml in the Y axis and minutes after glucose load in minutes in the X axis. Values were expressed as mean +SEM. (#P < 0.05). E, Insulin release area under curve (AUC) values were presented as µU/ml min-1 in the Y axis and expressed as mean +/-SEM (*P < 0.05) for each group presented in the X axis. Data obtained (mean +SEM/SD): Sham 1: 2589 + 390.5/952.82; Sham 2: 2902.5 + 401.3/979.17; RYGB: 4676.25 + 490.23/1196.16; PdIT: 3661.19 + 420.12/1025.09.

group nine weeks after surgery. Fig. 3A shows that Shams and PdIT rats showed similar plasma GIP glucose patterns throughout the assay. However, RYGB resulted in an increased secretion pattern at 60, 105, and 120 min (#P < 0.05). Moreover, RYGB animals displayed a significant increase in plasma GIP AUC with respect to Sham1, Sham 2 and PdIT animals (*P < 0.05) (Fig. 3B).

Regarding the plasma GLP-1 measurement, we observed a significantly increased GLP-1 secretion pattern after a mixed meal in RYGB and PdIT rats with respect to control rats throughout the assay (# P < 0.05) (Fig. 3C). This situation also appeared when we observed the plasma GLP-1 AUC in Fig. 3D. Thus, RYGB and PdIT exhibited higher AUC values with respect to the Sham 1 and Sham 2 groups (*P < 0.05).

3.3. Pancreatic beta-cell mass, GIP/ GLP-1 intestinal expression and Islet size distribution

The Pancreatic beta-cell mass was calculated in every animal in each group (Sham 1, Sham 2, RYGB and PdIT) using total pancreas weight and the insulin-positive area/total pancreatic area ratio. Fig. 4A shows significant increases in beta-cell mass in RYGB but also in PdIT-operated animals with respect to the Sham group (*P < 0.05). In addition, a small but significant difference also appears between RYGB and PdIT beta-cell mass (*P < 0.05).

The histomorphometric study revealed an increase in the percentage of small islets in the interval between 20 and 100 µm2 in animals subjected to RYGB but not in the other groups (*P < 0.05).

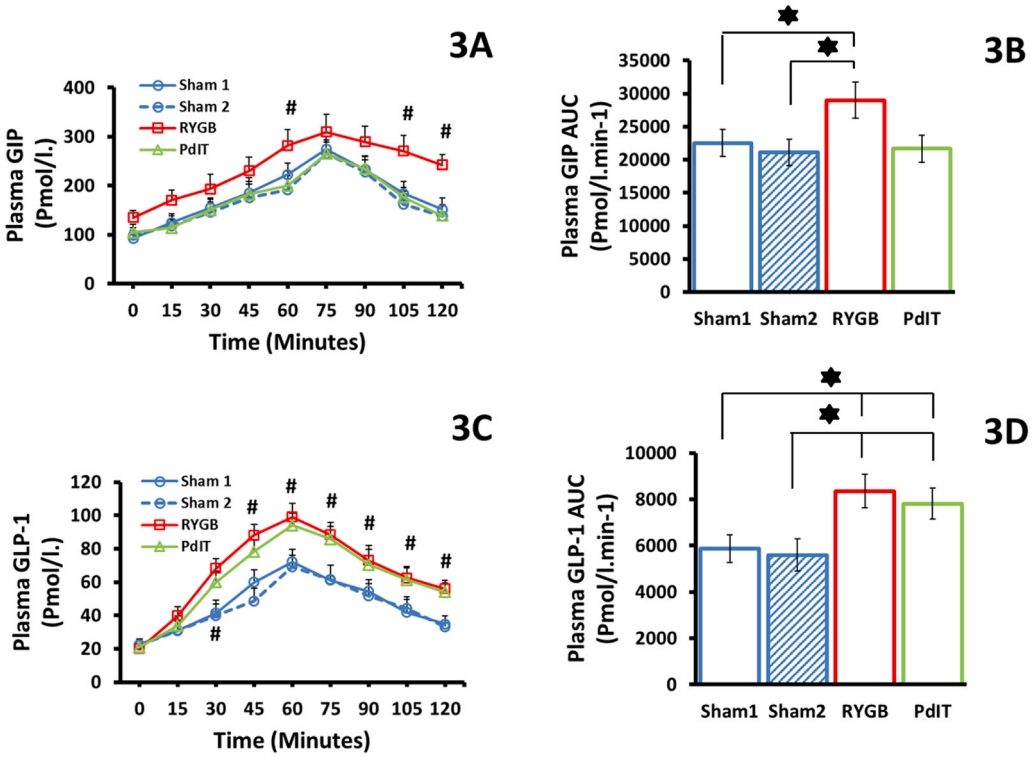

Fig. 3. Hormonal determinations. A. GIP secretion pattern after mixed meal administration. GIP plasma levels were represented as pmol/ml in the Y axis and time in minutes after mixed meal load in the X axis. Values were expressed as mean +SEM (#P < 0.05). B. Plasma GIP secretion area under curve (AUC) values were presented as pmol/ml min-1 in the Y axis and expressed as mean+ SEM (*P < 0.05) for each group presented in the X axis. Data obtained (mean +SEM/SD): Sham 1: 22,534.5 + 2067.9/5045.67; Sham 2: 21,096.75 + 1998.7/4876.82; RYGB: 29,013 + 2744.2/6695.84; PdIT: 21,666 + 2011.3/4907.57. C. GLP-1 secretion pattern after mixed meal administration. GLP-1 plasma levels were represented as pmol/ml in the Y axis and time in minutes after mixed meal load in the X axis. Values were expressed as mean +SEM (#P < 0.05). D, Plasma GLP-1 secretion area under curve (AUC) values were presented as pmol/ml min-1 in the Y axis and expressed as mean +SEM (*P < 0.05) for each group presented in the X axis. Data obtained (mean +SEM/SD): Sham1: 5862.6 + 599.1/1461.80; Sham 2: 5598.37 + 690.2/13660.02; RYGB: 8354.1 + 720.78/1758.70; PdIT: 7817.175 + 660.1/1610.64.

Also a significant decreased percentage of islets between 300 and 400 μm^2 in RYGB animal respect controls as shown in Fig. 4D.

In duodenum and ileum samples from each group, GIP- and GLP-1-positive cell numbers were tested using immunostaining, and a similar number of GIP-positive cells were found in the Shams and PdIT groups. However, a high increase in GIP-producing cells was registered in RYGB-operated rats with respect to the controls and PdIT animals (*P < 0.05) (Fig. 4B).

When we tested the number of GLP-1-positive cells in the ileum from the animals of each group, we observed (as shown in Fig. 4C) an approximately two-fold increase in the number of GLP-1-producing cells in RYGB and PdIT-operated rats with respect to Sham 1 and Sham 2-operated animals (**P < 0.01).

3.4. Relative effects of surgeries on glucose metabolism

To facilitate the identification of the duodenal exclusion effect and early ileal stimulation, we relativized the effect of each surgery to 0 with respect to the control group (Sham 1) and expressed it as a percentage of the effect on beta-cell mass and insulin response.

As shown in Fig. 5A, RYGB provides further beta-cell mass growth, which was approximately 37,01 % more than PdIT, while PdIT shows 62,99 % more than the Sham 1 procedure (control). Fig. 5B shows a one-fold increase in insulin response in RYGB rats with respect to PdIT animals and a 51,2 % increase in the insulin response in PdIT-operated rats with respect to the control.

4. Discussion

The beneficial impact of RYGB on T2DM before the onset of significant weight loss has long been reported in patients (Kashyap et al., 2010). In this sense, many authors accept that the main factors involved in this phenomenon are beyond weight loss and decreased hepatic insulin resistance associated with weight loss (Han et al., 2022; Pérez-Arana et al., 2021). In order to isolate the mechanisms involved in the resolution of diabetes after bariatric surgery from those phenomena derived from subsequent weight loss, such as decreased insulin resistance, we decided to use healthy non-obese rodents in our study.

The role of GLP-1 in the underlying mechanism after surgery has long been established (Aminian et al., 2021; Jirapinyo et al., 2018). However, RYGB is a complex intervention that implies an early stimulation of the ileum but also duodenal segment exclusion. The effect of the latter on the entero-insular axis is less studied, which is probably due to the difficulty of separating ileal effects and duodenal effects. For this purpose, we used a preduodenal ileal transposed model that exhibits early ileal stimulation but also a duodenal flux of nutrients to compare with the RYGB rat model.

Regarding functional data, we observed no changes in glucose patterns after the OGTT in RYGB or PdIT animals with respect to Sham controls, as shown in Fig. 2B. These data were expected, considering that surgeries were performed on healthy Wistar rats and data were collected over the short term (twelve weeks), i.e., the aim was not to determine the degree of improvement of T2DM provided by each surgery. Instead, we focused the study on the changes underlying pathophysiological mechanisms of the entero-pancreatic axis after surgeries. Therefore, a healthy model allows us to avoid pathological interferences such as insulin resistance.

Despite this, significant differences were observed in the insulin response after the glucose challenge between Sham controls and RYGB or PdIT but also between RYGB and PdIT-operated animals (Fig. 2D and E), which indicated a different effect of both surgeries

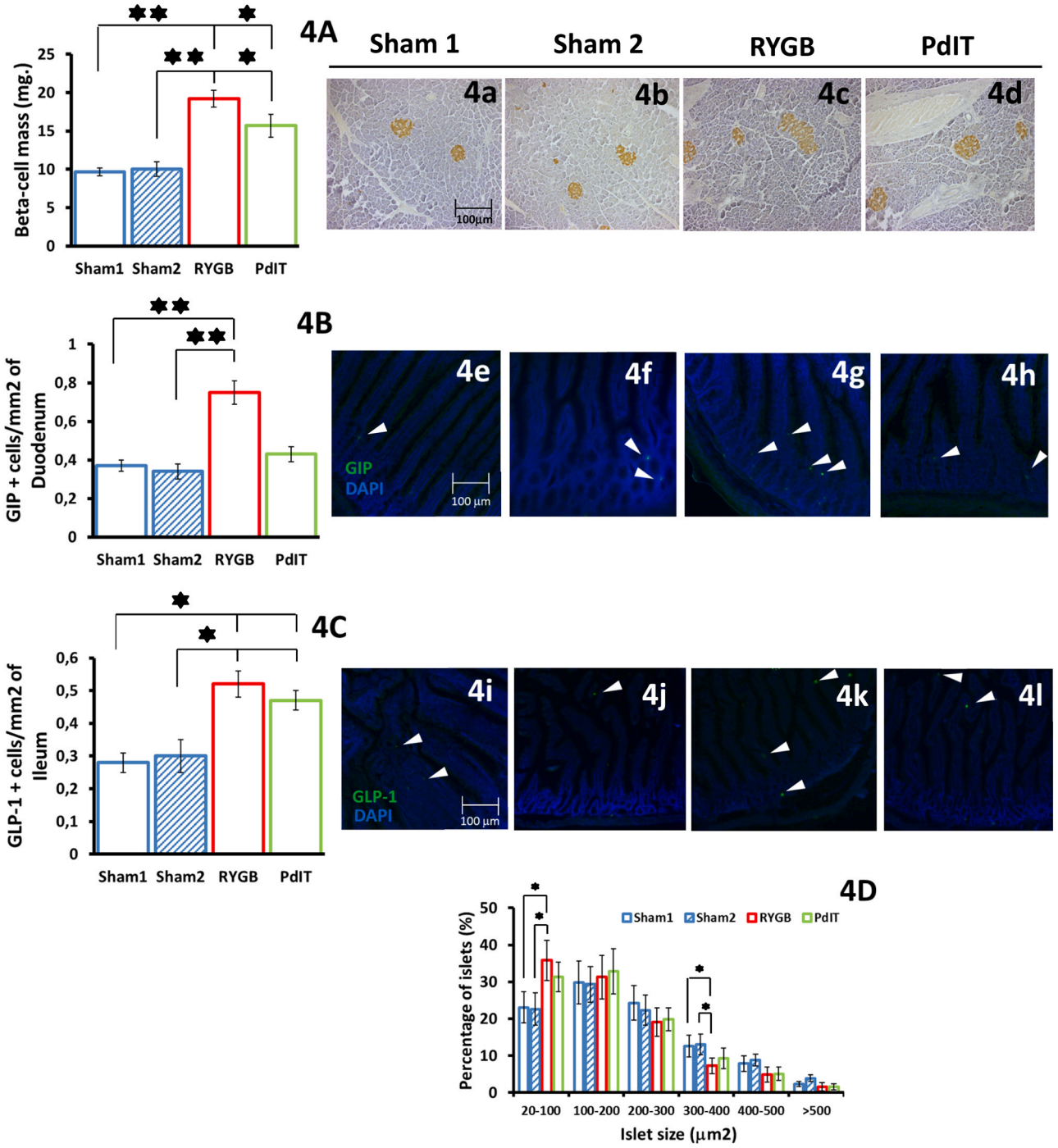

Fig. 4. Pancreatic beta-cells mass, GIP/GLP-1 intestinal expression and pancreatic islet size. A. Pancreatic beta-cell mass as mg. In the Y axis values were noted as the mean ± SEM (*P < 0.05, **P < 0.01) for each group to study: Sham 1, (blue bar), Sham 2 (Striped blue bar), RYGB (red bar) and PdIT (green bar). Data obtained (mean +SEM/SD): Sham 1: 9.67 + 0.5/1.22; Sham 2: 10.04 + 0.93/2.26; RYGB: 19.21 + 1.07/2.61; PdIT: 15.68 + 1.51/3.68. B: GIP expression in the duodenum as percentage of GIP positive cells/mm^2 of duodenum in the Y axis, values were noted as the mean ± SEM (*P < 0.05, **P < 0.01) for each group to study. Data obtained (mean +SEM/SD): Sham 1: 0.37 + 0.03/0.07; Sham 2: 0.34 + 0.04/0.09; RYGB: 0.75 + 0.06/0.14; PdIT: 0.43 + 0.04/0.09. C: GLP-1 expression in the ileum as percentage of GLP-1 positive cells/mm^2 of ileum in the Y axis, values were noted as the mean ± SEM (*P < 0.05) for each group to study. Data obtained (mean +SEM/SD): Sham 1: 0.28 + 0.03/0.07; Sham 2: 0.3 + 0.05/0.12; RYGB: 0.52 + 0.04/0.09; PdIT: 0.47 + 0.03/0.07. D: Size distribution of pancreatic islets expressed as percentage of islets (in the Y axis) in each size interval represented in the X axis (µm^2). Images 4a to 4c: pancreatic islets observed in pancreas samples from Sham 1 (4a), Sham 2 (4b), RYGB (4c) and PdIT animals (4d) using insulin immunostaining revealed with DAB (x20). Images 4e to 4h: duodenal expression of GIP in Sham 1 (4e), Sham 2 (4f) RYGB (4g) and PdIT (4h) using GIP immunostaining revealed with Alexa-488 (Green) and DAPI to counterstain nuclei (Blue). Images 4i to 4l: ileal expression of GLP-1 in Sham 1(4i), Sham 2 (4j), RYGB (4k) and PdIT (4l) using GLP-1 immunostaining revealed with Alexa-488 (Green) and DAPI to counterstain nuclei (Blue).

on beta-cell mass activity. These findings are consistent with those previously described for RYGB and ileal transposition surgeries (Mosinski et al., 2021; Patriti et al., 2007). Thus, regarding RYGB and PdIT plasma insulin AUC (Fig. 2E), we observed a stronger effect of RYGB on the insulin response. These data indicate a possible differential effect of both surgeries on pancreatic beta-cell mass. Surprisingly, an increased beta-cell mass was detected in the RYGB and PdIT groups due to the increase in the number of small islets, probably by neogenesis, at least in RYGB animals. (Fig. 4A and D). As in the study of insulin response, the highest beta-cell mass value was

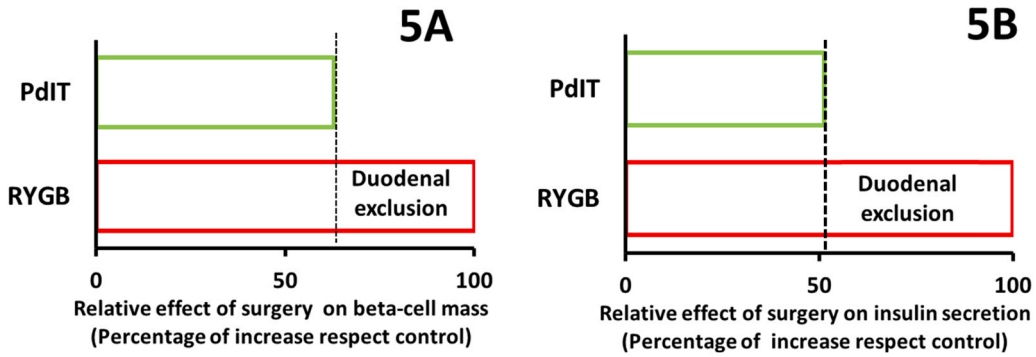

Fig. 5. Relative effects of surgeries on glucose metabolism. A in the X axis, percentage of relative effect of RYGB and PdIT on beta-cell mass (relativized to 0 with the control groups Sham 1/2). B in the x axis, percentage of relative effect of RYGB and PdIT on insulin secretion (relativized to 0 with the control groups Sham 1/2).

described for RYGB animals. Thus, both parameters are widely measured in RYGB and ileal transposition rodent models (Ahn et al., 2020; Zhang et al., 2017). However, our work provides a comparative scale of effects in the same model and in the same experiment (Fig. 5A and B).

These data imply some differential effects on the endocrine pancreas during RYGB surgery. This is in part due to early ileal stimulation and also due to duodenal exclusion, which is nonexistent in PdIT animals. To test our hypothesis, we studied the plasma secretion pattern after mixed-meal administration of two incretin hormones as follows: GIP, which is mostly secreted by K cells in the duodenum, and GLP-1, which is mostly secreted by L-cells in the ileum. According to a previous study (Camacho, et al., 2020), an elevated plasma GIP secretion pattern and a high plasma GIP AUC value were described by RYGB rats but not by PdIT or Sham-operated controls (Fig. 3A and B). These data could be controversial because many authors have proposed a decrease in plasma GIP values after RYGB (Zhou et al., 2015). However, these studies were performed on mice, and GIP secretion variability after RYGB between species, including humans, is commonly described (Lindqvist et al., 2017; Moran-Atkin et al., 2013). Our data confirmed the effect of duodenal exclusion on GIP secretion. Additionally, GIP tissue expression was tested, and a high number of GIP-producing cells were found in the duodenum from RYGB but not from PdIT-operated animals (Fig. 4B).

However, when we measured plasma levels of GLP-1 after mixed-meal administration, no difference was detected between RYGB and PdIT rats (Fig. 3C and D), and GLP-1 ileal expression values were also similar (Fig. 4C). This result was probably due to the presence of early stimulation of the ileum after both surgeries and agrees with the results proposed by other authors (Gaitonde et al., 2012; Ji et al., 2021).

Collectively, these data indicate two different effects of RYGB on the entero-insular axis. One effect, due to ileal stimulation and GLP-1 secretion, was responsible for 51,2 % of the insulin response and 62,99 % of the beta-cell mass increment after surgery (Fig. 5A and B), and the other, due to duodenal exclusion and increased GIP secretion, was responsible for 48,8 % of the insulin response and 37,01 % of the beta-cell mass increment after RYGB in our model. Therefore, our data emphasize the importance of duodenal exclusion and GIP secretion on glucose metabolic changes after RYGB. Moreover, this dual activity on the entero-insular axis derived from RYGB surgery could explain some paradoxical situations, such as those described by Mokadem et al. (2013), where RYGB surgery improved glucose homeostasis in GLP-1 K.O. mice. In fact, GIP has been proposed not only as an insulinotropic agent (Gault et al., 2003), but also as a synergistic agent with GLP-1 (Samms et al., 2020), and dual agonists have been developed for T2DM treatment (Frías, 2020). Our data confirm these synergistic effects on insulin release but also on beta-cell mass increase. Thus, we must not neglect the role of GIP versus GLP-1 when we study the long-term pathophysiological mechanisms after RYGB and T2DM relapse. In addition, a deeper acknowledgement of the role of each incretin hormone after every bariatric/metabolic surgery variant could facilitate the use of mixed pharmacological and surgical treatments and allow less harmful and more efficient surgical procedures for T2DM treatment.

CRediT authorship contribution statement

A Camacho, G Pérez-Arana and JA Prada designed the project and followed the financially the project. D Almorza and I Mateo analysed the procedures for statistical analysis. A Diaz, A Camacho, A Ribelles, M Gracia and MJ Castro performed the surgical techniques, followed the animal survival period and performed the functional test. G Pérez-Arana directed and measured the histological techniques with A Diaz, A Ribelles and M Gracia. All the authors participated in preparing the manuscript.

Declaration of Competing Interest

The authors declare that they have no known competing financial interests or personal relationships that could have appeared to influence the work reported in this paper.

Acknowledgment and grant support

The authors desire to thank Ms. Sofie Winderick for the technical support at the Department of anatomy laboratory. We thank the support of *Tugiana Peal of Becerra Association*. The authors declare the research project was supported by University of Cadiz and Institute for Biomedical Science Research and Innovation (INIBICA).

References

Ahn, C.H., Choi, E.H., Oh, T.J., Cho, Y.M., 2020. Ileal Transposition increases pancreatic β cell mass and decreases β cell senescence in diet-induced obese rats. Obes. Surg. 30 (5), 1849–1858. https://doi.org/10.1007/s11695-020-04406-6

Aminian, A., Wilson, R., Zajichek, A., Tu, C., Wolski, K.E., Schauer, P.R., Kattan, M.W., Nissen, S.E., Brethauer, S.A., 2021. Cardiovascular outcomes in patients with type 2 diabetes and obesity: comparison of gastric bypass, sleeve gastrectomy, and usual care. Diabetes Care 44 (11), 2552–2563. https://doi.org/10.2337/dc20-3023

Arterburn, D.E., Telem, D.A., Kushner, R.F., Courcoulas, A.P., 2020. Benefits and risks of bariatric surgery in adults: a review. JAMA 324 (9), 879–887. https://doi.org/10.1001/jama.2020.12567

Camacho-Ramírez, A., Prada-Oliveira, J.A., Ribelles-García, A., Almorza-Gomar, D., Pérez-Arana, G.M., 2020. The leading role of peptide tyrosine tyrosine in glycemic control after Roux-en-Y Gastric bypass in rats. Obes. Surg. 30 (2), 697–706.

Frías, J.P., 2020. Tirzepatide: a glucose-dependent insulinotropic polypeptide (GIP) and glucagon-like peptide-1 (GLP-1) dual agonist in development for the treatment of type 2 diabetes. Expert Rev. Endocrinol. Metab. 15 (6), 379–394. https://doi.org/10.1080/17446651.2020.1830759

Gaitonde, S., Kohli, R., Seeley, R., 2012. The role of the gut hormone GLP-1 in the metabolic improvements caused by ileal transposition. J. Surg. Res 178 (1), 33–39. https://doi.org/10.1016/j.jss.2011.04.044

Gault, V.A., O'Harte, F.P., Flatt, P.R., 2003. Glucose-dependent insulinotropic polypeptide (GIP): anti-diabetic and anti-obesity potential? Neuropeptides 37 (5), 253–263. https://doi.org/10.1016/j.npep.2003.09.002

Han, L., Z,hang, T., You, D., Chen, W., Bray, G., Sacks, F., Qi, L., 2022. Temporal and mediation relations of weight loss, and changes in insulin resistance and blood pressure in response to 2-year weight-loss diet interventions: the POUNDS Lost trial. Eur. J. Nutr. 61 (1), 269–275. https://doi.org/10.1007/s00394-021-02643-8

Ji, Y., Lee, H., Kaura, S., Yip, J., Sun, H., Guan, L., Han, W., Ding, Y., 2021. Effect of bariatric surgery on metabolic diseases and underlying mechanisms. Biomolecules 11 (11), 1582. https://doi.org/10.3390/biom11111582

Jirapinyo, P., Jin, D.X., Qazi, T., Mishra, N., Thompson, C.C., 2018. A meta-analysis of GLP-1 After Roux-En-Y Gastric Bypass: impact of surgical technique and measurement strategy. Obes. Surg. 28 (3), 615–626. https://doi.org/10.1007/s11695-017-2913-1

Kalinowski, P., Paluszkiewicz, P., Wróblewski, T., Remiszewski, P., Grodzicki, M., Bartoszewicz, Z., Krawczyk, M., 2017. Ghrelin, leptin, and glycemic control after sleeve gastrectomy versus Roux-en-Y gastric bypass-results of a randomized clinical trial. Surg. Obes. Relat. Dis. 13 (2), 181–188. https://doi.org/10.1016/j.soard.2016.08.025

Kashyap, S.R., Daud, S., Kelly, K.R., Gastaldelli, A., Win, H., Brethauer, S., Kirwan, J.P., Schauer, P.R., 2010. Acute effects of gastric bypass versus gastric restrictive surgery on beta-cell function and insulinotropic hormones in severely obese patients with type 2 diabetes. Int. J. Obes. 34 (3), 462–471. https://doi.org/10.1038/ijo.2009.254

Lindqvist, A., Ekelund, M., Pierzynowski, S., Groop, L., Hedenbro, J., Wierup, N., 2017. Gastric bypass in the pig increases GIP levels and decreases active GLP-1 levels. Peptides 90, 78–82. https://doi.org/10.1016/j.peptides.2017.02.009

Liu, Y., Zhou, Y., Wang, Y., Geng, D., Liu, J., 2011. Roux-en-Y gastric bypass induced improvement of glucose tolerance and insulin resistance in type 2 diabetic rats are mediated by glucagon-like peptide-1. Obes. Surg. 21 (9), 1424–1431.

Lupi, R., Del Guerra, S., D'Aleo, V., Boggi, U., Filipponi, F., Marchetti, P., 2010. The direct effects of GLP-1 and GIP, alone or in combination, on human pancreatic islets. Regul. Pept. 2–3, 129–132. https://doi.org/10.1016/j.regpep.2010.04.009

Miskelly, M.G., Shcherbina, L., Thorén Fischer, A.H., Abels, M., Lindqvist, A., Wierup, N., 2021. GK-rats respond to gastric bypass surgery with improved glycemia despite unaffected insulin secretion and beta cell mass. Peptides 136, 170445 . https://doi.org/10.1016/j.peptides.2020.170445

Mokadem, M., Zechner, J.F., Margolskee, R.F., Drucker, D.J., Aguirre, V., 2013. Effects of Roux-en-Y gastric bypass on energy and glucose homeostasis are preserved in two mouse models of functional glucagon-like peptide-1 deficiency. Mol. Metab. 3 (2), 191–201.

Moran-Atkin, E., Brody, F., Fu, S.W., Rojkind, M., 2013. Changes in GIP gene expression following bariatric surgery. Surg. Endosc. 27 (7), 2492–2497. https://doi.org/10.1007/s00464-012-2764-8

Mosinski, J.D., Aminian, A., Axelrod, C.L., Batayyah, E., Romero-Talamas, H., Daigle, C., Mulya, A., Scelsi, A., Schauer, P.R., Brethauer, S.A., Kirwan, J.P., 2021. Roux-en-Y gastric bypass restores islet function and morphology independent of body weight in ZDF rats. Am. J. Physiol. Endocrinol. Metab. 320 (2), E392–E398. https://doi.org/10.1152/ajpendo.00467

Patriti, A., Aisa, M.C., Annetti, C., Sidoni, A., Galli, F., Ferri, I., Gullà, N., Donini, A., 2007. How the hindgut can cure type 2 diabetes. Ileal transposition improves glucose metabolism and beta-cell function in Goto-kakizaki rats through an enhanced Proglucagon gene expression and L-cell number. Surgery 142 (1), 74–85. https://doi.org/10.1016/j.surg.2007.03.001

Pérez-Arana, G., Díaz, A., Bancalero, J., Camacho, A., Fernández, J., Ribelles, A., Almorza, D., Carrasco, C., Mateo, I., Prada-Oliveira, J.A., 2021. The long-term failure of RYGB surgery in improving T2DM is related to hyperinsulinism. Ann. Anat. 240, 151855 . https://doi.org/10.1016/j.aanat.2021.151855

Piteau, S., Olver, A., Kim, S.J., Winter, K., Pospisilik, J.A., Lynn, F., Manhart, S., Demuth, H.U., Speck, M., Pederson, R.A., 2007. Reversal of islet GIP receptor down-regulation and resistance to GIP by reducing hyperglycemia in the Zucker rat. Biochem. Biophys. Res. Commun. 362, 1007–1012. https://doi.org/10.1016/j.bbrc.2007.08.115

Rahman, R., Azagury, D.E., 2017. Novel technologies and techniques in bariatric surgery. Minerva Chir. 72 (2), 125–139. https://doi.org/10.23736/S0026-4733.16.07265-5

Samms, R.J., Coghlan, M.P., Sloop, K.W., 2020. How may GIP enhance the therapeutic efficacy of GLP-1? Trends Endocrinol. Metab. 31 (6), 410–421. https://doi.org/10.1016/j.tem.2020.02.006

Schauer, P.R., Bhatt, D.L., Kirwan, J.P., S.T.A.M.P.E.D.E. Investigators, 2017. Bariatric surgery versus intensive medical therapy for diabetes 5-year outcomes. N. Engl. J. Med. 376, 641–651.

Zhang, S., Guo, W., Wu, J., Gong, L., Li, Q., Xiao, X., Zhang, J., Wang, Z., 2017. Increased β-cell mass in obese rats after gastric bypass: a potential mechanism for improving glycemic control. Med. Sci. Monit. 23, 2151–2158. https://doi.org/10.12659/msm.902230

Zhou, J., Hao, Z., Irwin, N., Berthoud, H.R., Ye, J., 2015. Gastric inhibitory polypeptide (GIP) is selectively decreased in the roux-limb of dietary obese mice after RYGB surgery. PLoS One 10 (8), e0134728 . https://doi.org/10.1371/journal.pone.0134728